

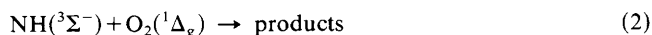
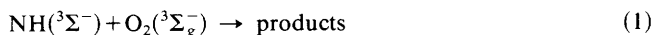
Reaction of $\text{NH}(X^3\Sigma^-)$ with $\text{O}_2(^3\Sigma_g^-)$ and $\text{O}_2(^1\Delta_g)$ in the Gas Phase

BY WALTER HACK,* HARTMUT KURZKE AND HEINZ GEORG WAGNER

Max-Planck-Institut für Strömungsforschung, Böttingerstrasse 4-8, 3400 Göttingen, Federal Republic of Germany

Received 17th September, 1984

The reactions



have been studied in an isothermal discharge-flow reactor with resonance absorption (H, O) and laser-induced fluorescence (OH, NH) detection methods. The NH radicals were produced *via* $\text{F} + \text{NH}_3 \rightarrow \text{NH}_2 + \text{HF}$ and $\text{NH}_2 + \text{F} \rightarrow \text{NH} + \text{HF}$. The $\text{O}_2(^1\Delta_g)$ source was either a chemical generator [$\text{Cl}_2 + \text{H}_2\text{O}_2 \rightarrow \text{O}_2(^1\Delta_g) + 2\text{HCl}$] or a microwave discharge in O_2 . For reaction (1) a pressure-independent ($1.2 \leq p/\text{mbar} \leq 10.5$) rate constant:

$$k_1(T) = 7.6 \times 10^{10} \exp(-6.4 \pm 0.6 \text{ kJ mol}^{-1}/RT) \text{ cm}^3 \text{ mol}^{-1} \text{ s}^{-1}$$

was determined in the temperature range $286 \leq T/\text{K} \leq 543$. For reaction (2) an upper limit for the rate constant:

$$k_2(295 \text{ K}) = (6 \pm 1) \times 10^9 \text{ cm}^3 \text{ mol}^{-1} \text{ s}^{-1}$$

was obtained at room temperature. The mechanisms of reaction (1) and (2) are discussed.

The $\text{NH}(X^3\Sigma^-)$ radical is an important intermediate in NH-containing combustion systems since its reactions significantly influence the fate of the nitrogen ending up as N_2 or NO_x .

The number of direct investigations on the reactivity of the $\text{NH}(^3\Sigma^-)$ radical is low,¹ although it is of considerable interest for the modeling of ammonia + oxygen flames² as well as atmospheric chemistry. Among these reactions the elementary step with the oxidizer O_2 has to be emphasized. For the same reason special attention has to be paid to the reaction



in atmospheric photochemistry. NH radicals are known to be a major NH_3 photolysis product at short wavelengths ($\lambda \leq 147 \text{ nm}$), a fact which underlines the importance of NH radical reactions.

The rate constant for reaction (1) at room temperature has been measured by Zetsch and Hansen³ using a pulsed vacuum u.v. photolysis of mixtures containing NH_3 , O_2 and He. The concentration of NH radicals has been followed by resonance fluorescence of $\text{NH}(A^3\Pi - X^3\Sigma)$. They determined the rate constant at room temperature without identifying the primary products. No other results of this reaction have been published, and in particular the temperature dependence, which is of essential importance for atmospheric modeling, has not yet been determined directly.

The products of reaction (1) have been discussed theoretically by Melius and Binkley.⁴ The products $\text{NO}_2(\tilde{X}^2A_1) + \text{H}(^2S)$ or $\text{NO}(^2\Pi) + \text{OH}(^2\Pi)$ correlate *via* the

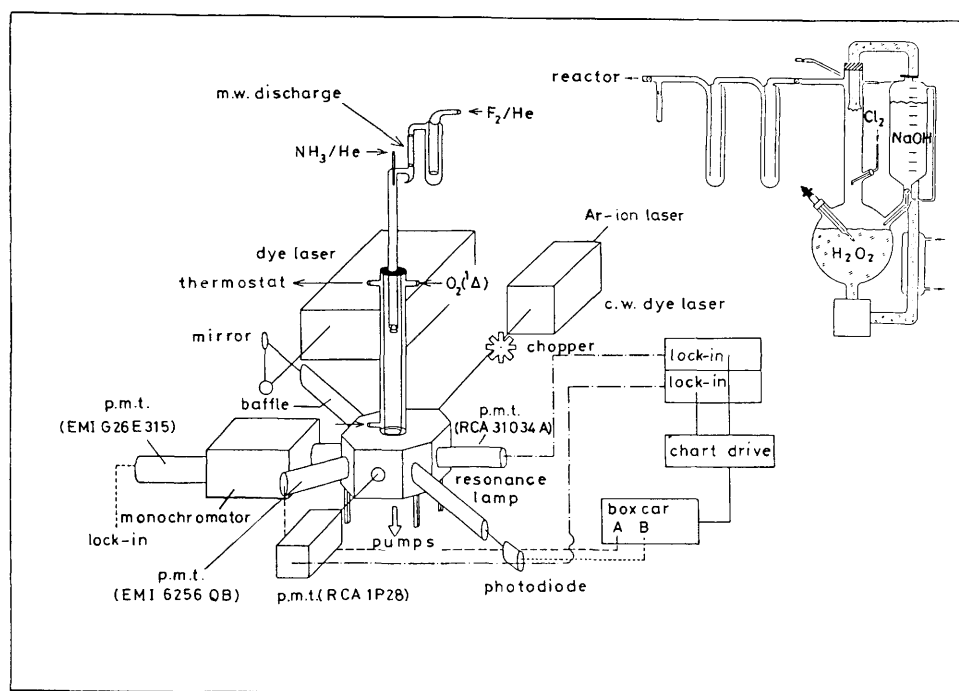
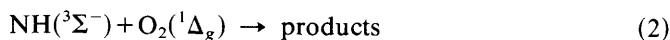


Fig. 1. Schematic diagram of the experimental set-up and the O₂(¹Δ_g) generator.

(¹A') surface whereas the products HNO(³A'') + O(³P) correlate adiabatically *via* the lowest (³A') surface. For the reaction with electronically excited oxygen:



the lowest adiabatic surface could be a (³A') surface. The energy available is sufficient to populate another state (³A'') of the HNOO intermediate.⁴ Neither the rate nor the products of reaction (2) have been studied directly.

The object of this work is to study the temperature dependence of the rate, $k_1(T)$, and determine the primary products of reaction (1) and to measure the rate and determine the products of reaction (2).

EXPERIMENTAL

APPARATUS AND MATERIALS

The experimental apparatus is shown schematically in fig. 1. The main features and more details have been described in previous publications.⁵⁻⁷ All experiments were carried out in isothermal flow reactors made of Pyrex glass. The inner wall of the flow tube was coated with halocarbon wax⁸ (halocarbon wax 15-00, Halocarbon Corporation, N.J.) for temperatures up to 353 K. For temperatures > 353 K Teflon FEP (856-200) varnish was chosen (Du Pont de Nemours). Two reactors with different inside diameters, 3.6 cm (surface/volume = $s/v = 1.1 \text{ cm}^{-1}$) and 5.6 cm ($s/v = 0.7 \text{ cm}^{-1}$), were used to examine the effect of surface reactions. Time resolution was achieved by means of a moveable probe made of quartz. At a constant flow velocity the reaction time was calculated from the difference between the point of detection and the nozzle of the probe. This distance could be varied between 11 and 65 cm.

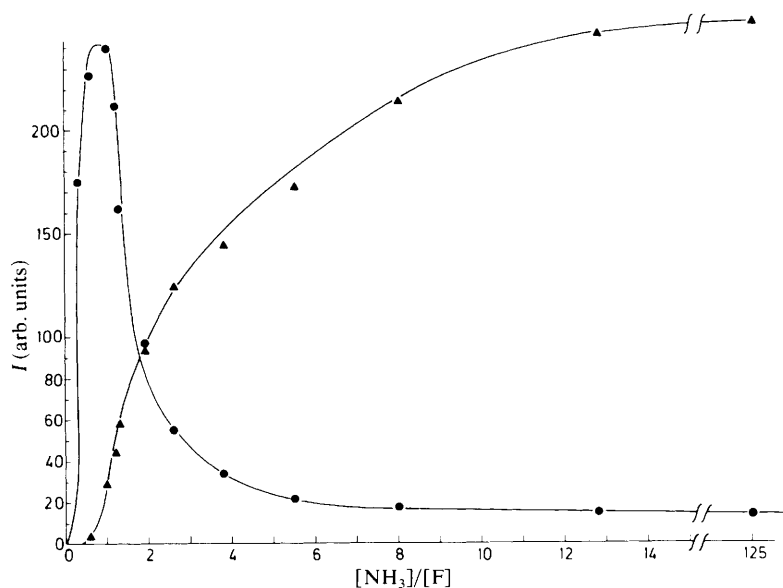


Fig. 2. Plot of the production of NH(●) and NH₂(▲) radicals against the ratio $[\text{NH}_3]/[\text{F}]$. $[\text{F}_2]_0 = 1.6 \times 10^{-12} \text{ mol cm}^{-3}$, $t_R = 40 \text{ ms}$.

The $\text{NH}(X^3\Sigma^-)$ radicals were produced in the moveable probe by the fast reactions⁹



under the conditions $0.7 \leq [\text{NH}_3]/[\text{F}_2] \leq 3$. This $\text{F} + \text{NH}_3$ reaction system was studied in a separate experiment in greater detail (fig. 2). At a fixed reaction time of 40 ms and a constant F_2 concentration of $1.6 \times 10^{-12} \text{ mol cm}^{-3}$, the relative concentrations of NH and NH_2 radicals were measured as a function of the $[\text{NH}_3]/[\text{F}_2]$ ratio in the range $0.3 \leq [\text{NH}_3]/[\text{F}] \leq 125$. A microwave discharge in a $\text{F}_2 + \text{He}$ mixture gives F atoms. Traces of water were removed by passing the mixture through three liquid N_2 traps, one attached directly to the discharge cavity. The $\text{NH}_3 + \text{He}$ mixture was introduced through the inner tube of the probe. This arrangement provided a constant $[\text{NH}]_0$ at the tip of the probe. The flow conditions inside the probe were adjusted to allow complete consumption of F atoms.

Helium was used as the main carrier gas. For all gases the highest commercially available purity was used. In addition, oxygen was further purified by passing it through a liquid- N_2 trap. The main gas flow was pumped off with a $250 \text{ m}^3 \text{ h}^{-1}$ pump. A small portion of the gas enters the detection cell through a glass skimmer ($\phi = 1.5 \text{ mm}$). To avoid the effect of pressure dependence on the fluorescence intensity, the pressure in the detection cell was chosen independently of the flow system (0.26 mbar). The detection cell was pumped out by a $350 \text{ m}^3 \text{ h}^{-1}$ Roots pump.

DETECTION SYSTEMS

The concentrations of H and O atoms were measured with a pulsed resonance-absorption device, usually working at 250 Hz. The detection limit for this technique was determined with the titration reactions $\text{N} + \text{NO} \rightarrow \text{N}_2 + \text{O}$ and $\text{H} + \text{NO}_2 \rightarrow \text{OH} + \text{NO}$ to be $[\text{O}] \geq 5 \times 10^{-15}$ and $[\text{H}] \geq 3 \times 10^{-15} \text{ mol cm}^{-3}$, respectively. The radiation of the resonance lamp (mW discharge in He, $P_L = 0.65 \text{ mbar}$) was focussed on the entrance slit of a 20 cm monochromator (Acton Research model VM-502) after passing through the absorption volume. The resonance

radiation was detected with a solar-blind p.m.t. (E.M.I. model G 26E315) feeding a lock-in amplifier.⁶

OH and NH radicals were detected with a pulsed, flashlamp-pumped dye laser (Chromatix model CMX-4) at 308.2 nm for OH [$P_1(1)$ line of the (0, 0) band, $^2\Sigma^+ - ^2\Pi$ transition] and at 336 nm for NH [Q (0, 0) line, $^3\Pi^- - ^3\Sigma$ transition]. The detection limits are [OH] $\geq 4 \times 10^{-17}$ and [NH] $\approx 1 \times 10^{-18}$ mol cm⁻³ determined by the titration $H + NO_2 \rightarrow OH + NO$. For NH the sensitivity was estimated from production in the system $F + NH_3$. The integral radical fluorescence was observed perpendicularly to the laser beam with a p.m.t. (H.T.V. model R-955), driving channel A of a boxcar-averager (Parc model 162). The laser intensity was monitored with a photodiode connected to channel B. NH₂ radicals were measured with a c.w. dye laser as described previously¹⁰ with the detection limit [NH₂] $\geq 1 \times 10^{-16}$ mol cm⁻³ estimated in the same way as in previous publications. The detection limit for HNO (\tilde{X}^1A'') by LIF was [HNO] $\geq 2 \times 10^{-13}$ mol cm⁻³. The absolute O₂($^1\Delta_g$) concentration was measured by photoionisation with an Ar resonance lamp (LiF window) relative to NO($X^2\Pi$).

To provide optimum isolation from shocks and vibration the whole apparatus was seated on an air-suspended laser table.

THE O₂($^1\Delta_g$) SOURCE

O₂($^1\Delta_g$) was produced either in a microwave discharge in pure O₂¹¹ or using a chemical generator.⁶ Both methods were used in order to have a comparison between the results, cancelling out any effects caused by the method of production.

In a glass flow system 1.8 dm³ of alkaline 85% H₂O₂ was circulated with a 40 dm³ min⁻¹ rotary pump. The temperature was maintained at -1 °C to avoid unwanted decomposition of H₂O₂. Cl₂ was introduced into the flow system through a small tube. The surface reaction of Cl₂ with alkaline H₂O₂ yielded O₂($^1\Delta_g$) concentrations up to 35% at a pressure of 5.2 mbar. This yield was limited only by the size of the tubing. A cold trap at dry-ice temperature was inserted into the flow path to freeze out the H₂O coming out of the reactor.

The most frequently used technique to produce O₂($^1\Delta_g$) using a microwave discharge in O₂ yielded only 4.4% of singlet oxygen. The O atoms were destroyed by passing the gas stream over a layer of freshly prepared HgO. With our resonance-absorption device we were not able to detect any O atoms coming out of the discharge, *i.e.* [O] $\leq 5 \times 10^{-15}$ mol cm⁻³.

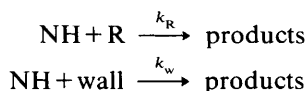
CONDITIONS

Measurements were carried out in the temperature range $268 \leq T/K \leq 543$ and in the pressure range $1.3 \leq P/\text{mbar} \leq 10.5$. The average linear-flow velocity was in the range $930 \leq v/\text{cm s}^{-1} \leq 2200$, resulting in reaction times from 5 to 70 ms.

The ratio [NH₃]/[F₂] ranged from 0.7 to 3, whereas the maximum NH concentration was achieved at the ratio [NH₃]/[F₂] = 0.7. Under these conditions the concentration of NH₂ was negligible (fig. 2). The initial concentration of ammonia was in the range $5.1 \times 10^{-13} \leq [\text{NH}_3]/\text{mol cm}^{-3} \leq 3.2 \times 10^{-12}$ and that of fluorine in the range $3.8 \times 10^{-13} \leq [\text{F}_2]/\text{mol cm}^{-3} \leq 4.6 \times 10^{-12}$. The corresponding concentration of molecular oxygen was in the range $6.8 \times 10^{-10} [\text{O}_2]/\text{mol cm}^{-3} \leq 1.22 \times 10^{-8}$ and that of O₂($^1\Delta_g$) was varied in the range $1.5 \times 10^{-10} \leq [\text{O}_2(^1\Delta_g)]/\text{mol cm}^{-3} \leq 3.48 \times 10^{-9}$. We did not attempt to determine the absolute concentration of NH since the sources available for a calibration are not precise enough. All concentration profiles of NH are relative.

ANALYSIS OF THE DATA

The NH concentration profiles were measured under pseudo-first-order conditions for [NH]₀ \ll [O₂($^3\Sigma_g^-$)] and [NH]₀ \ll [O₂($^1\Delta_g$)]₀. For the reaction scheme



the following differential equation is obtained:

$$-d[\text{NH}]/dt = k_w[\text{NH}] + k_R[\text{NH}][\text{R}]$$

where $[\text{R}]$ stands for the sum of all reactants present in excess over NH :

$$[\text{R}] = \sum_{i=1}^n [\text{R}_i].$$

The reaction of NH with itself, which is second order in NH , can be neglected since the initial NH concentration was so small ($[\text{NH}]_0 < 10^{-12} \text{ mol cm}^{-3}$). The pseudo-first-order reactions are summed as

$$k_{\text{eff}} = \sum_{i=1}^n k_i[\text{R}_i]$$

giving the definition of k_{eff} and leading to

$$-d[\text{NH}]/dt = k_w[\text{NH}] + k_{\text{eff}}[\text{NH}].$$

Furthermore, the wall rate constant k_w and k_{eff} can be summed to give k_{exp} , which is observed experimentally as

$$-d[\text{NH}]/dt = k_{\text{exp}}[\text{NH}]$$

leading to

$$\Delta \ln ([\text{NH}]/[\text{NH}]_0) = k_{\text{exp}} \Delta t.$$

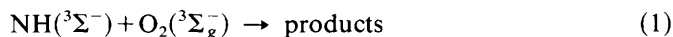
The rate constant k_w for the removal of NH without adding O_2 to the system was determined before and after every series of measurements. The limitations of this method have been discussed previously.⁸

RESULTS

The rate constants were obtained from the NH profiles in the presence of an excess of $\text{O}_2(^3\Sigma_g^-)$ and $\text{O}_2(^1\Delta_g)$ over $[\text{NH}]_0$. The determination of the products is described below.

REACTION RATES

The rate of the reaction



was obtained from plots of $\ln \text{NH}$ against Δt , as shown in fig. 3. Under all the experimental conditions linear first-order plots for the decay of NH radicals were obtained (fig. 3). The rate for wall removal of NH ($18 \leq k_w/s^{-1} \leq 50.4$) is higher than the values measured by Zetzsch and Stuhl,¹² increasing with the temperature of the reactor wall (table 1). There is no dependence of k_w on the initial F_2 concentration, which is a measure for the NH yield, nor on the ratio $[\text{NH}_3]/[\text{F}_2]$. The reaction of NH with NH_2 , which is known to be very fast,¹³ is of no importance under our experimental conditions since it is included in k_w . At a ratio $[\text{NH}_3]/[\text{F}_2] = 0.7$ the concentration of NH_2 is small (fig. 2), *i.e.* in the range $1 \times 10^{-14} \leq [\text{NH}_2]/\text{mol cm}^{-3} \leq 8 \times 10^{-14}$, the ratio of NH over NH_2 is in the range $3 \leq [\text{NH}]/[\text{NH}_2] \leq 40$. For this ratio only a rough estimate can be given since the absolute NH concentrations are not given to high accuracy.

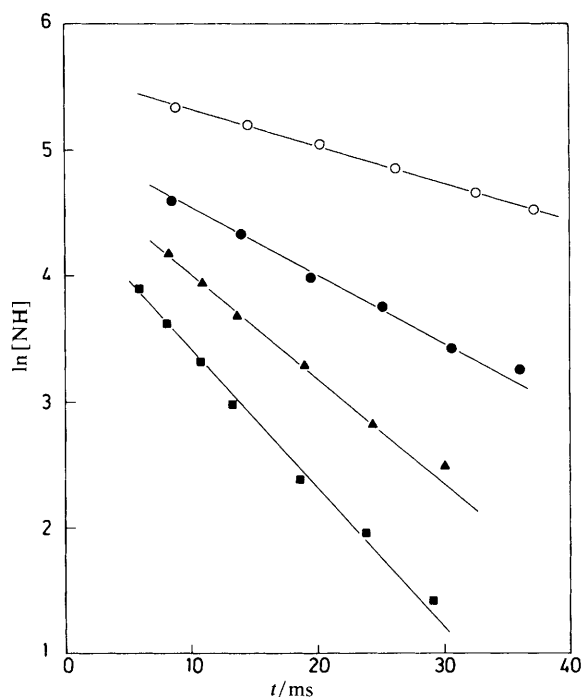


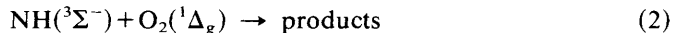
Fig. 3. First-order plot of the decay of $\text{NH}(X^3\Sigma^-)$ radicals in the presence and absence of $\text{O}_2(^3\Sigma_g^-)$. $T = 464\text{ K}$ and $P = 2.6\text{ mbar}$. $[\text{O}_2]/10^{-9}\text{ mol cm}^{-3}$: \circ , 0; \bullet , 1.9; \blacktriangle , 3.5; \blacksquare , 4.9.

Upon addition of $\text{O}_2(^3\Sigma_g^-)$ to the system, depletion of NH along the reaction path increased markedly. This increase varied linearly with the concentration of O_2 (fig. 3). From the semilogarithmic plots of the relative NH concentrations against the reaction time, first-order rate constants for the removal of NH by O_2 could be extracted. A plot of these rate constants against the O_2 concentration gave a value for the second-order rate constant for reaction (1) (fig. 4). These measurements were carried out for six different temperatures ($268 \leq T/\text{K} \leq 543$, fig. 5 and table 2) resulting in the following Arrhenius expression:

$$k_1(T) = 7.6 \times 10^{10} \exp[-(6.4 \pm 0.6)\text{ kJ mol}^{-1}/RT] \text{ cm}^3 \text{ mol}^{-1} \text{ s}^{-1}.$$

In the pressure range $1.3 \leq P/\text{mbar} \leq 10.5$ there was no dependence of the rate on pressure.

In order to study the rate of the reaction



the $\text{O}_2(^3\Sigma_g^-)$ was partly converted into $\text{O}_2(^1\Delta_g)$ by microwave discharge or a mixture of $\text{O}_2(^3\Sigma_g^-)$ and $\text{O}_2(^1\Delta_g)$ coming out of the chemical reactor was mixed with $\text{NH}(^3\Sigma^-)$. The addition of $\text{O}_2(^1\Delta_g)$ to the system ($1.5 \times 10^{-10} \leq [\text{O}_2(^1\Delta_g)]/\text{mol cm}^{-3} \leq 3.48 \times 10^{-9}$) did not result in a significant change in the concentration profiles of NH compared with those in the absence of $\text{O}_2(^1\Delta_g)$. At an $\text{O}_2(^3\Sigma_g^-)$ concentration of $9.9 \times 10^{-9}\text{ mol cm}^{-3}$ and a corresponding $\text{O}_2(^1\Delta_g)$ concentration of $3.5 \times 10^{-9}\text{ mol cm}^{-3}$, using the chemical generator, the observed change in the NH concentration profile did not exceed 10%. Obviously $\text{O}_1(^1\Delta_g)$ is reacting neither faster

Table 1. Experimental results for the reaction $\text{NH} + \text{O}_2(^3\Sigma) \rightarrow \text{products}$

T/K	P/mbar	$[\text{F}_2]_0/10^{12} \text{ mol cm}^{-3}$	$[\text{NH}_3]/[\text{F}_2]$	$[\text{O}_2]/10^{-9} \text{ mol cm}^{-3}$	k_w/s^{-1}	$k_{\text{eff}}/\text{s}^{-1}$
268	2.6	1.5	0.8	2.3	18	8
268	2.6	1.5	0.8	4.2	18	19
268	2.6	1.5	0.8	6.3	18	26
268	2.6	1.5	0.8	8.3	18	35
268	2.6	1.5	0.8	9.8	18	42
268	2.6	1.5	0.8	11.7	18	46
295	1.3	1.7	0.9	1.95	24.4	11
295	1.3	1.7	0.9	2.7	24.4	14.6
295	2.6	3.7	0.7	3.9	22	19
295	2.6	3.7	0.7	6.1	22	30
295	2.6	3.7	0.7	8.2	22	45
295	2.6	3.7	0.7	9.8	22	55
295	10.5	4.6	0.7	3	21	19.4
295	10.5	4.6	0.7	6	21	32
295	10.5	4.6	0.7	8	21	49.3
295	10.5	4.6	0.7	1	21	57.7
295	10.5	4.6	0.7	1.22	21	62.1
353	2.6	1.1	0.7	0.68	25	8
353	2.6	1.1	0.7	1.5	25	24
353	2.6	1.1	0.7	2.5	25	27
353	2.6	1.1	0.7	4	25	31
353	2.6	1.1	0.7	5.2	25	43
353	2.6	1.1	0.7	7.2	25	59
398	2.6	0.99	0.7	1	20.3	12
398	2.6	0.99	0.7	2.1	12	22.4
398	2.6	0.99	0.7	2.8	12	30.7
398	2.6	0.99	0.7	3.3	12	34.7
398	2.6	0.99	0.7	4.1	12	42.4
398	2.6	0.99	0.7	4.9	12	58
464	2.6	0.38	3	1.4	28	19.7
464	2.6	0.38	3	1.9	28	27.3
464	2.6	0.38	3	2	28	32
464	2.6	0.38	3	3.5	28	51.5
464	2.6	0.38	3	4.9	28	82
543	2.6	0.73	0.7	0.8	50.4	16.4
543	2.6	0.73	0.7	1.1	50.4	18
543	2.6	0.73	0.7	1.7	50.4	31.6
543	2.6	0.73	0.7	2.2	50.4	42.8
543	2.6	0.73	0.7	3.3	50.4	60.8

nor substantially slower at room temperature than $\text{O}_2(^3\Sigma_g^-)$. From this observation we obtained an upper limit for the rate of reaction (2):

$$k_2(295 \text{ K}) = (6 \pm 1) \times 10^9 \text{ cm}^3 \text{ mol}^{-1} \text{ s}^{-1}.$$

This value comes from the $[\text{O}_2(^1\Delta_g)]/[\text{O}_2(^3\Sigma_g^-)]$ ratio and the assumption that a 10% change in the NH profile would have been observed.

The results have been treated using the least-squares method. For reaction (1) there is an uncertainty of $\pm 10\%$. The estimated error for the determination of the upper limit for the rate constant of reaction (2) is 20%, mainly because of the uncertainty in the measurements of the absolute $\text{O}_2(^1\Delta)$ concentration.

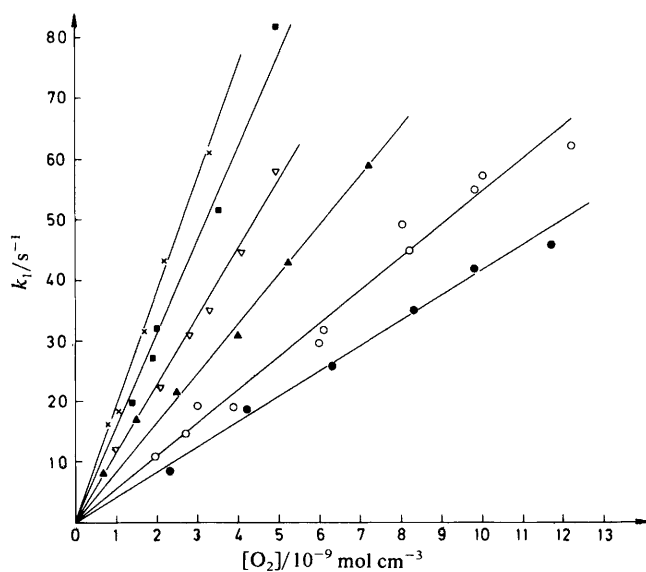
GAS-PHASE REACTION OF NH WITH O₂

Fig. 4. Plot of pseudo-first-order rate constants for reaction (1) against O₂(³Σ_g⁻) concentration.
 T/K: ●, 268; ○, 295; ▲, 353; ▽, 398; ■, 464; ×, 543.

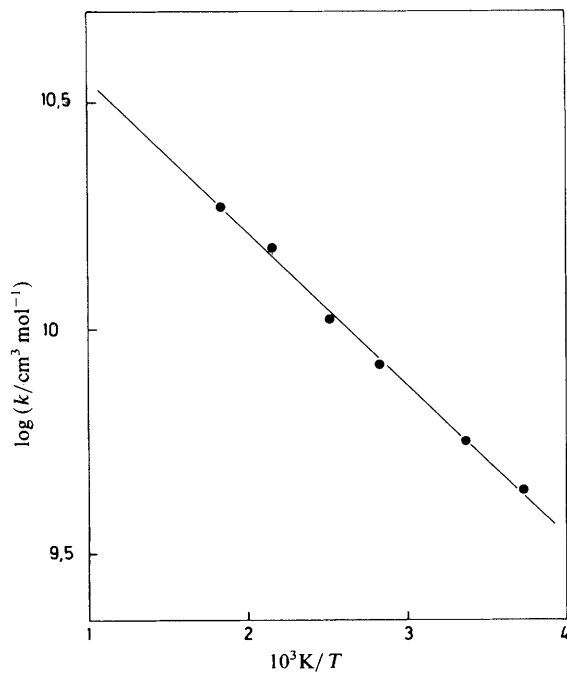
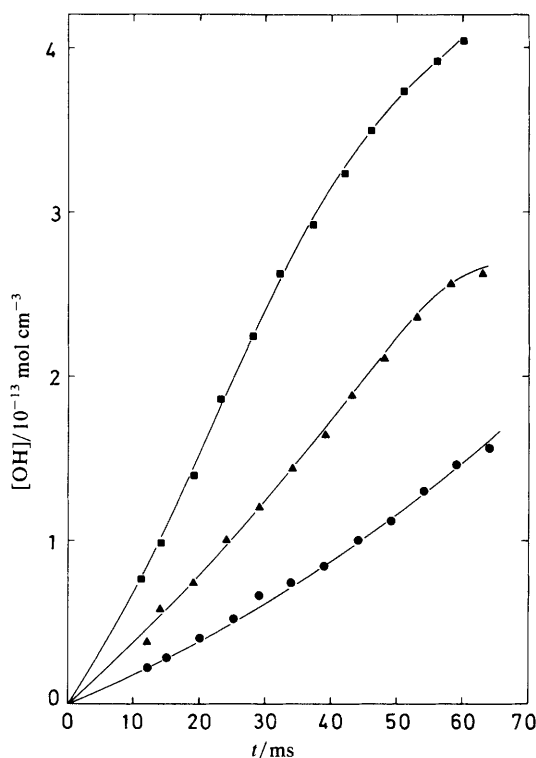


Fig. 5. Arrhenius plot for reaction (1).

Table 2. Temperature dependence of the rate constant of reaction (1)

T/K	$k_1/10^9 \text{ cm}^3 \text{ mol}^{-1} \text{ s}^{-1}$
268	4.4
295	5.5
353	8.3
398	10.5
464	15
543	18.6

**Fig. 6.** Plot of the production of OH radicals in reaction (1) against time. $T = 295 \text{ K}$ and $P = 2.6 \text{ mbar}$. $[\text{O}_2(^3\Sigma_g^-)]/10^{-9} \text{ mol cm}^{-3}$: ●, 1.9; ▲, 4.1; ■, 8.1.

REACTION PRODUCTS

To obtain the products of reaction (1) and (2) the profiles of several atoms and radicals expected as products were recorded. Under the same experimental conditions used for the determination of the rate constant of reaction (1), the concentration profiles of OH radicals were recorded. The measured OH profiles for three different $\text{O}_2(^3\Sigma_g^-)$ concentrations are shown in fig. 6. The absolute concentration of OH radicals together with the rate constant obtained from the initial slope of the profiles indicates that OH is the main product of reaction (1) under these experimental

conditions. The OH sensitivity was calibrated by means of the reaction



We did not monitor NO since the lower-wavelength limit of the laser is at 265 nm. Neither for reaction (1) nor for reaction (2) could H or O atoms be detected as a product. The sensitivity of our l.i.f. arrangements is not expected to be sufficient for the detection of HNO(\tilde{X}^1A') radicals at the initial NH concentrations used in this study.

The products of reaction (2) were observed using the same techniques and in similar concentration ranges as described above. Upon addition of O₂($^1\Delta_g$) to the system the profiles of the OH radicals did not change within experimental error. In reaction (2) products other than those of reaction (1) were not found.

DISCUSSION

The source of NH radicals is the reaction



and the fast consecutive reaction



where $k_3 = 2 \times 10^{13} \text{ cm}^3 \text{ mol}^{-1} \text{ s}^{-1}$ and $k_4 \approx 2 \times 10^{13} \text{ cm}^3 \text{ mol}^{-1} \text{ s}^{-1}$.⁹ Besides the NH($X^3\Sigma^-$) radical, the reaction of fluorine atoms with ammonia at ratios $[\text{NH}_3]/[\text{F}_2] < 1$ should give rise to different radicals and atoms in subsequent steps of the reaction.⁹ At higher ratios (> 5) the main product will be NH₂, whereas all other radicals are of minor importance. The maximum in the production of NF radicals is situated at $[\text{NH}_3]/[\text{F}_2] \approx 0.3$.¹⁴ This may also be the case for N atoms. In this region significant production of H atoms can be observed, possibly from the reaction



Under our experimental conditions the concentration of each of these radicals and atoms seems to be negligible. The first-order plots did not give any hint of interfering secondary reactions resulting in a deviation from linearity. The rates of the reactions of NH₂, N and H with O₂ are too slow to compete with the reaction of NH radicals. Neither the decay of NH in the presence of oxygen nor the observed OH radicals can be explained by a reaction other than reaction (1). The presence of NF radicals can be checked easily by introducing O₂($^1\Delta_g$) into the system. If NF is present a bright green chemiluminescence is observed, as described in ref. (14).

Electronically excited NH($a^1\Delta$, $b^1\Sigma$), which may be formed in reaction (4), will be deactivated during the long residence time inside the probe ($t_R \geq 30 \text{ ms}$).

For the reaction



a room-temperature value of $k_1(296 \text{ K}) = (5.1 \pm 0.5) \times 10^9 \text{ cm}^3 \text{ mol}^{-1} \text{ s}^{-1}$ was obtained by Zetzsch and coworkers¹ in a pulsed vis.-u.v. photolysis ($\lambda \geq 105 \text{ nm}$) system containing NH₃, O₂ and He at *ca.* 1 bar total pressure. The authors pointed out that other reactive species and also electronically excited O atoms could be present in the vis.-u.v. photolysis system but no effect of these species was observed. This assumption is supported by our observations since the chemical source used in our experiment excludes the presence of most of the species mentioned by Zetzsch and

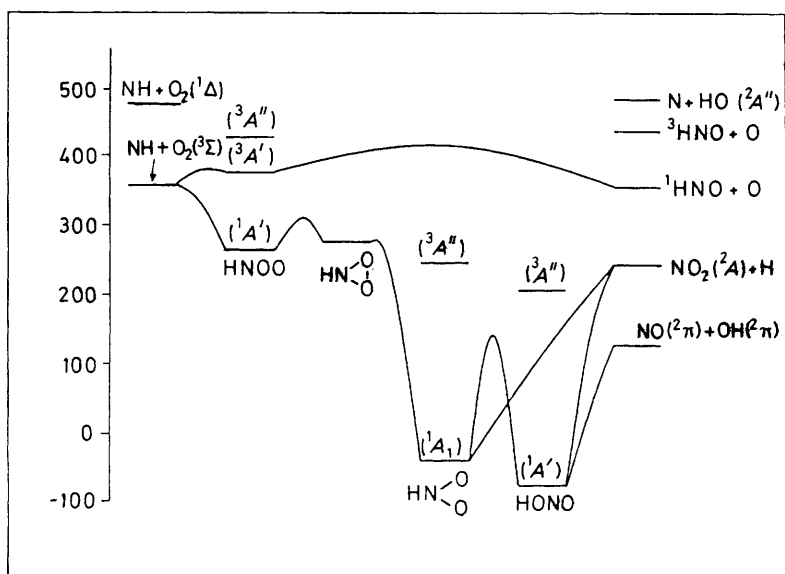
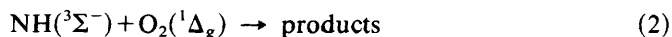
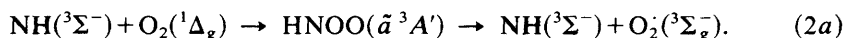


Fig. 7. Calculated energies of possible intermediates and products for the reaction of $\text{NH} + \text{O}_2$ [see ref. (4)].

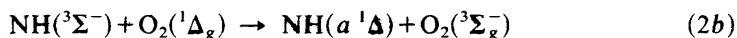
For the reaction



physical quenching is possible *via* the $\text{HNOO}(^3A')$ intermediate:



The energy-transfer reaction



is endothermic with $\Delta H_R = 56 \text{ kJ mol}^{-1}$ and can thus be neglected near room temperature.

The chemical products of reaction (2) which are energetically possible are those available for $\text{NH}(^3\Sigma^-) + \text{O}_2(^3\Sigma_g^-)$ and in addition $\text{HNO}(\tilde{a}^3A'') + \text{O}(^3P)$. In our experiment the quenching process has not been studied. The addition of $\text{O}_2(^1\Delta_g)$ to our reaction system seems to have no influence on the observed rate constant for $\text{NH}(^3\Sigma_g^-)$ depletion nor on the product distribution. Changes in the profiles of NH and OH radicals are within experimental error. The O and $\text{HNO}(\tilde{X}^1A')$ concentrations were below the detection limit in the presence of $\text{O}_2(^1\Delta_g)$. Emission of $\text{HNO}(\tilde{A}^1A'')$, which is known to be formed by energy transfer in the $\text{HNO} + \text{O}_2(^1\Delta_g)$ system,¹⁶ was not observed. These results can be understood either if there is a significant barrier to form $(\text{HNO}_2)^*$ in the $\text{NH}(^3\Sigma_g^-) + \text{O}_2(^1\Delta_g)$ or more likely if reaction 2(a) is much faster than a chemical reaction. The difference in the rate for reaction (2) compared with reaction (1) can be explained by the different energy hypersurfaces involved in the reaction of $\text{O}_2(^3\Sigma_g^-)$ and $\text{O}_2(^1\Delta_g)$. Following the calculations by Binkley and Melius the lowest triplet surface is not accessible for reaction (2), since it will lead to avoided curve-crossing of the potential surfaces.

For this reason reaction (2) should have a large activation barrier, forming the HNO_2 intermediate on a higher triplet surface.

- ¹ I. Hansen, K. Höinghaus, C. Zetzsch and F. Stuhl, *Chem. Phys. Lett.*, 1976, **42**, 370.
- ² J. A. Miller, M. D. Smooke, R. M. Green and R. J. Kee, *Kinetic Modeling of the Oxidation of Ammonia in Flames*, paper no. WSS/C182-93, presented at the Western States Fall Sectional Meeting of the Combustion Institute, Livermore, California, Sandia report, SAND 82-86009, 1983.
- ³ C. Zetzsch and I. Hansen, *Ber. Bunsenges. Phys. Chem.*, 1978, **82**, 830.
- ⁴ J. S. Binkley and C. F. Melius, *Oxidation of the NH and NH₂ Radicals*, paper no. WSS/CI 82-96, Fall Meeting of the Western States Section of the Combustion Institute, Livermore, California, 1982; C. F. Melius and J. S. Binkley, *ACS Symp. Ser.*, 1984, **249**.
- ⁵ W. Hack, O. Horie and H. Gg. Wagner, *Ber. Bunsenges. Phys. Chem.*, 1981, **85**, 72.
- ⁶ W. Hack, H. Kurzke and H. Gg. Wagner, *Bericht Nr. 9/1983* Max-Planck-Institut für Strömungsforschung.
- ⁷ W. Hack and H. Kurzke, *Chem. Phys. Lett.*, 1984, **104**, 93.
- ⁸ W. Hack, O. Horie and H. Gg. Wagner, *J. Phys. Chem.*, 1981, **86**, 765.
- ⁹ C. D. Walther and H. Gg. Wagner, *Ber. Bunsenges. Phys. Chem.*, 1983, **87**, 403.
- ¹⁰ G. Hancock, W. Lange, M. Lenzi and K. H. Welge, *Chem. Phys. Lett.*, 1975, **33**, 168.
- ¹¹ C. W. Bader and E. A. Ogryzlo, *Discuss. Faraday Soc.*, 1964, **37**, 46.
- ¹² C. Zetzsch and F. Stuhl, *Ber. Bunsenges. Phys. Chem.*, 1981, **85**, 564.
- ¹³ F. Temps, *Bericht Nr. 4/1983*, Max-Planck-Institut für Strömungsforschung.
- ¹⁴ W. Hack and O. Horie, *Chem. Phys. Lett.*, 1981, **82**, 327.
- ¹⁵ T. Böhlend, *Diplom. Thesis* (Universität Göttingen, 1984).
- ¹⁶ Y. Ishiwata and I. Tanaka, *J. Phys. Chem.*, 1978, **82**, 1336.

(PAPER 4/1609)